# Synthesis and Electrochemical Studies of Nickel Complexes with a Flexidentate Bipyridine-aza-crown Ether Ligand

Sebastian Acosta-Calle,<sup>†</sup> Elsa Z. Huebsch, <sup>†</sup> Jenna E. Halenda, Zoe E. Stuart, Chun-Hsing Chen, and Alexander J.M. Miller\*

Department of Chemistry, University of North Carolina at Chapel Hill, Chapel Hill, North Carolina 27599-3290, United States

#### Abstract

Bipyridine ligands have been extensively employed in nickel catalysis, with ligand modifications focused on steric or electronic tuning. In this work, we explore modifications designed to modulate the coordination mode using a 2,2'-bipyridine derivative with an appended aza-crown ether macrocycle capable of flexidentate binding to nickel. A series of complexes varying in charge from neutral to dicationic demonstrates the flexibility of the macrocycle, with bipyridine-aza-crown ether denticity changing from  $\kappa^4$  to  $\kappa^6$  upon sequential abstraction of chloride ligands. The changes in binding mode can be reversed by addition of chloride ion. Comparisons between the macrocycle-containing ligand and an analogous ligand with a non-macrocyclic diethylamine donor provide insight into the role of the crown ether, including in electrochemical reductions probed via cyclic voltammetry.

## Introduction

The venerable ligand 2,2'-bipyridine (bpy) and its derivatives have helped transform numerous fields of chemistry.<sup>1–4</sup> One important area is in nickel catalysis, where bipyridine ligands have supported an impressive diversity of reactivity, particularly in polymer and oligomer synthesis and in cross-coupling reactions under thermal, electrochemical, or

<sup>&</sup>lt;sup>†</sup> Denotes equal contribution

photochemical conditions.<sup>5–9</sup> In many cases the bpy ligands are proposed to aid in accessing multiple redox states through delocalization of charge into the low-lying  $\pi^*$  orbitals — bpy ligands are quintessential "redox active ligands".<sup>10,11</sup>

The coordination number and geometry of nickel bipyridine complexes strongly influence their redox activity. 12–15 An interesting opportunity emerges, therefore, in the design of responsive ligands that can access multiple binding modes or geometries through the use of chemical additives. To this end, we have prepared a derivative of 2,2'-bipyridine that contains an aza-crown ether macrocycle (**Figure 1**). We hypothesized that the ether groups could serve as hemilabile ligands to nickel, coordinating oxygen atoms as needed to complete an octahedral coordination environment. We have previously shown that addition of alkali metal cations to complexes with hemilabile crown ether ligands can modulate the coordination properties in complexes with limited redox activity. In nickel complexes with a bipyridine anchoring ligand, cation-crown interactions could reversibly alter the coordination mode and geometry of the ligand while retaining desired redox properties.

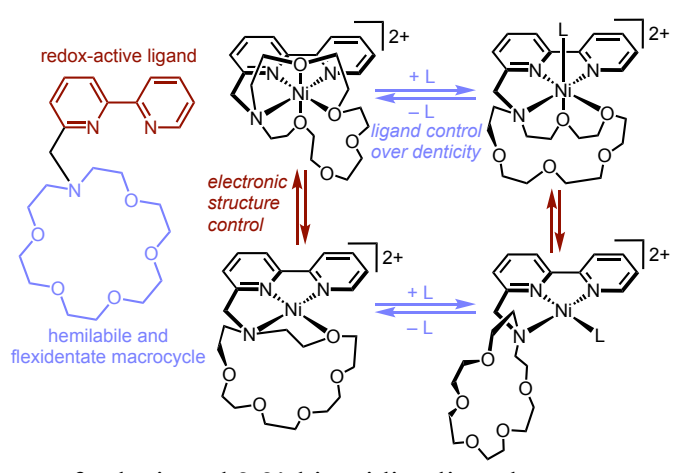


Figure 1. Design features of substituted 2,2'-bipyridine ligand to support variable denticity.

The use of cation-crown interactions for "tunable hemilability" has so far been focused on pincer ligands with the strong-field ligand aminophenylphosphinito (NCOP), which supports

diamagnetic complexes of iridium, nickel, and palladium with a range of cation-modulated coordination chemistry and catalysis. <sup>17–24</sup> The lack of well-defined redox activity in these systems led us to explore bipyridine-containing variants. It was not clear at the outset, however, whether nickel(II) complexes would adopt four-, five-, or six-coordinate structures, or whether the crown ether appended to bipyridine would readily adopt multiple binding modes.

Here we present a family of nickel complexes with 6-aminomethyl-2,2'-bipyridine (NNN) ligands featuring either diethylamine or aza-18-crown-6 ether. The aza-18-crown-6 ether macrocycle was selected based on our previous studies showing strong binding of alkali metal cations and flexible denticity. <sup>22,25</sup> Complexes of nickel(II) in four different binding modes, ranging from tridentate to hexadentate, have been synthesized and characterized, and the ability to reversibly switch between modes has been demonstrated. Comparisons between the two ligands reveal starkly different coordination chemistry and properties when the crown ether is present. The demonstrated flexidenticity and cation-crown interactions illustrate alternative strategies to exert control over the coordination environment of nickel bipyridine complexes, which could be leveraged in the rational design of redox active catalysts.

#### **Results and Discussion**

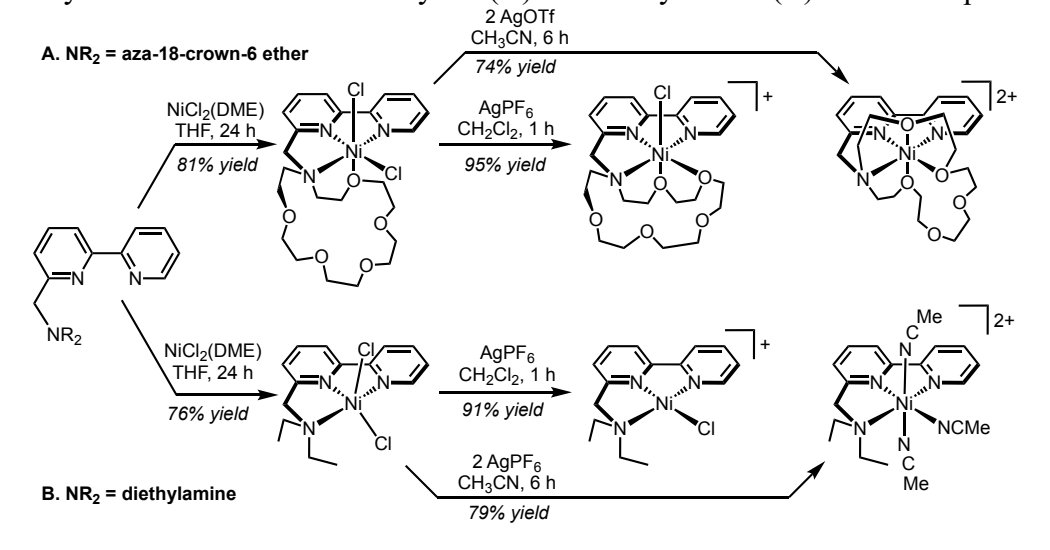
## Synthesis and characterization of nickel complexes

An alternative synthesis for the previously reported macrocycle-containing bpy ligand <sup>18c6</sup>NNN was developed via reductive amination of 6-formyl-2,2'-bipyridine with aza-18-crown-6 ether (a-18c6) in 90% yield (SI Scheme 1).<sup>26,27</sup> The <sup>1</sup>H NMR resonances were in good agreement with the literature, and characterization was augmented with <sup>13</sup>C NMR and mass spectrometry. A cyclic voltammogram of <sup>18c6</sup>NNN (SI Figure 18) produced a reversible reduction (–2.64 V vs

Fc<sup>+/0</sup>, Fc is ferrocene) similar to free bipyridine (-2.60 V vs. Fc<sup>+/0</sup>).<sup>28</sup> To our knowledge, no well-defined transition metal complexes of the <sup>18c6</sup>NNN ligand have been reported.

Metalation of <sup>18c6</sup>NNN with NiCl<sub>2</sub>(DME) (DME is 1,2-dimethoxyethane) afforded ( $\kappa^4$ <sup>18c6</sup>NNN)NiCl<sub>2</sub> as a green solid in 81% yield (Scheme 1A). Broad peaks ranging from 2 to 150 ppm in the <sup>1</sup>H NMR spectrum indicated the presence of a high-spin d<sup>8</sup> nickel complex. The solution magnetic moment obtained by the Evans method,  $\mu_{eff} = 2.89 \ \mu_B$ , is consitent with an S = 1 configuration (SI Equations 1-2, SI Figure 3).<sup>29</sup> Crystals grown from dichloromethane layered with diethyl ether were subjected to single-crystal X-ray diffraction (XRD) analysis, which established an octahedral coordination environment (Figure 2A). The <sup>18c6</sup>NNN ligand adopts a  $\kappa^4$  (tetradentate) binding mode with the chloride ligands in a cis orientation and a crown ether oxygen atom trans to one of the chloride ligands.

**Scheme 1.** Synthetic scheme for macrocyclic (A) and diethylamino (B) nickel complexes.



Treatment of  $(\kappa^4$ -18c6NNN)NiCl<sub>2</sub> with one equiv AgPF<sub>6</sub> afforded  $[(\kappa^5$ -18c6NNN)NiCl]<sup>+</sup> as a paramagnetic ( $\mu_{eff} = 3.08 \ \mu_B$ , Evans method) green compound in 95% yield (Scheme 1A). The pentadentate binding mode of the ligand was confirmed through an XRD study of crystals grown

from CH<sub>2</sub>Cl<sub>2</sub> layered with pentane, with adjacent crown ether oxygen atoms adopting a cis geometry trans to a pyrdine and chloride (**Figure 2B**).

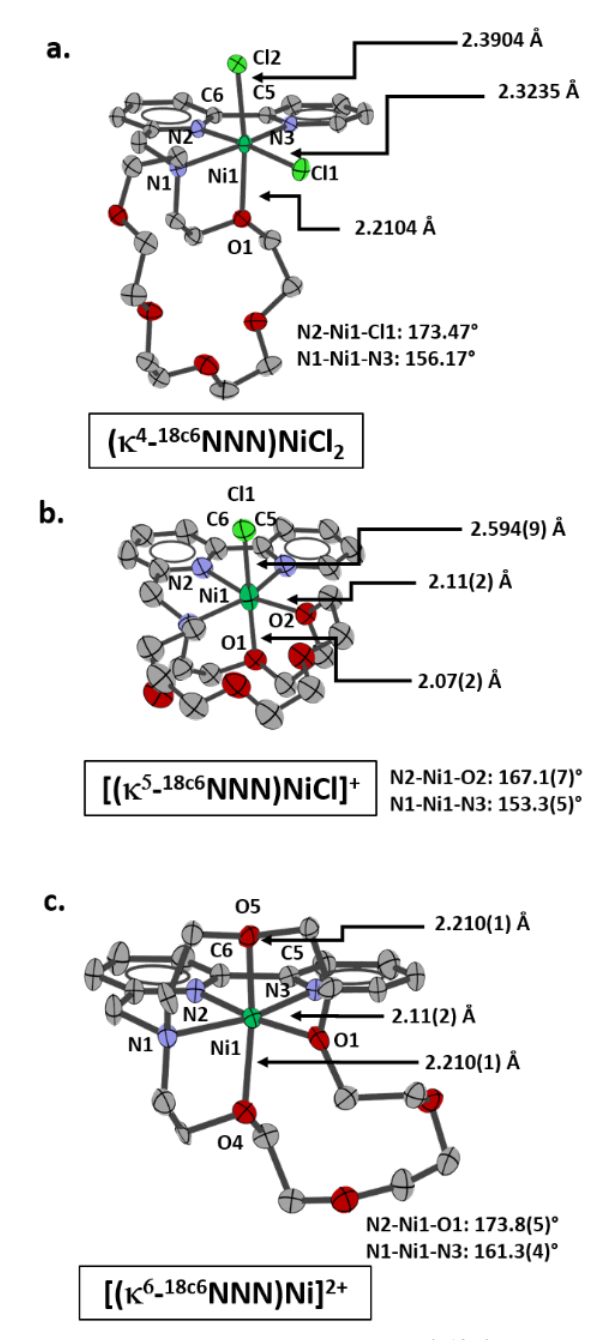


**Figure 2.** Structural representations of neutral  $(\kappa^{4-18c6}NNN)NiCl_2$  (a), cationic  $[(\kappa^{5-18c6}NNN)NiCl]^+$  (b), and dicationic  $[(\kappa^{6-18c6}NNN)Ni]^{2+}$  (c), with ellipsoids shown at 50% probability and hydrogen atoms and anions omitted. For **b** and **c**, disorder was successfully modeled and one of two sets of positions is drawn. See Supporting Information for full details.

Double halide abstraction was attempted next. Treating ( $\kappa^4$ \_18c6NNN)NiCl<sub>2</sub> with 2 equiv AgOTf in acetonitrile solvent produced a purple solid in 74% yield (Scheme 1A). Single crystals suitable for diffraction were grown from layering a dichloromethane solution with diethyl ether. XRD revealed the identity of the complex as  $[(\kappa^6$ \_18c6NNN)Ni]^{2+}, a distorted octahedral complex with three crown ether oxygen donors: the two adjacent ethers that donated in the monocationic complex being joined by one ether on the other side of the amine arm that curls to fill the remaining coordination site. Both the neutral and dicationic macrocyclic Ni complexes displayed interpyridine C5-C6 bond lengths consistent with a neutral bpy ligand chelated to a nickel(II) center.<sup>30,31</sup>

There are salient differences in the nickel coordination chemistry of the new bpy-based ligand and the prior NCOP ligand containing a macroycle. The NCOP ligand enforces low-spin square planar coordination, whereas the weaker-field NNN ligand enables access to high-spin octahedral nickel complexes.<sup>22,23,32,25</sup> As a result, the NNN ligand accesses higher denticity, including a hexadentate coordination mode that has never been observed with the NCOP ligands.

Next, a non-macrocyclic ligand was developed to compare the coordination chemistry of a bipyridine system without additional ether donors. A diethylamine-containing comparison ligand  $^{\text{Et}}$ NNN was synthesized and metalated with NiCl<sub>2</sub>(DME) to give  $(\kappa^3-^{\text{Et}}$ NNN)NiCl<sub>2</sub> as a brown solid in 76% yield (Scheme 1B). XRD analysis revealed a distorted square pyramidal  $(\tau_5 = 0.14)$  complex with the NNN ligand in a tridentate binding mode (Figure 3A).

Halide abstraction from  $(\kappa^3 - E^t NNN)NiCl_2$  was accomplished by addition of AgPF<sub>6</sub>, affording the cationic species  $[(E^t NNN)NiCl]^+$  (Scheme 1B). In contrast to the crown-containing analogue  $[(\kappa^5 - 18c^6 NNN)NiCl]^+$ , the <sup>1</sup>H NMR spectrum of  $[(\kappa^3 - E^t NNN)NiCl]^+$  is diamagnetic, with diastereotopic splitting of the methylene protons of the ethyl groups not present in the free ligand

spectra (**SI Figure 9**). Bright pink crystals grown from dichloromethane layered with diethyl ether diffracted X-rays nicely, establishing the structure as a square planar nickel complex with tridentate NNN binding and the remaining Cl atom occupying the same plane as the bipyridine framework (N2–Ni1–Cl1: 178.6(1)°, **Figure 3B**). Addition of MeCN to the square planar complex results in a color change from pink to green and dramatic broadening and shifting of the <sup>1</sup>H NMR signals, consistent with acetonitrile binding to form a high-spin d<sup>8</sup> octahedral nickel complex (**Scheme 2**).

Scheme 2. Acetonitrile binding to (EtNNN)Ni complexes.

Additional halide abstraction from  $(\kappa^3$ -EtNNN)NiCl<sub>2</sub> only proceeded in the presence of an externally added donor such as MeCN. When two equivalents of AgPF<sub>6</sub> were added to the neutral complex in acetonitrile solvent, a purple product was isolated in 79% yield (Scheme 1B). XRD of single crystals of  $[(\kappa^3$ -EtNNN)Ni(MeCN)<sub>3</sub>]<sup>2+</sup> grown from acetonitrile layered with diethyl ether (Figure 3C) revealed a distorted octahedral geometry similar to the macrocyclic variant, with three acetonitrile ligands in a meridional arrangement. The Ni–N bond distances of the pincer-nitrogens ranged from 1.982(5) Å (amine arm) to 2.190(6) Å (bipyridine) with a constrained pincer angle of 158.4° (Figure 3c).

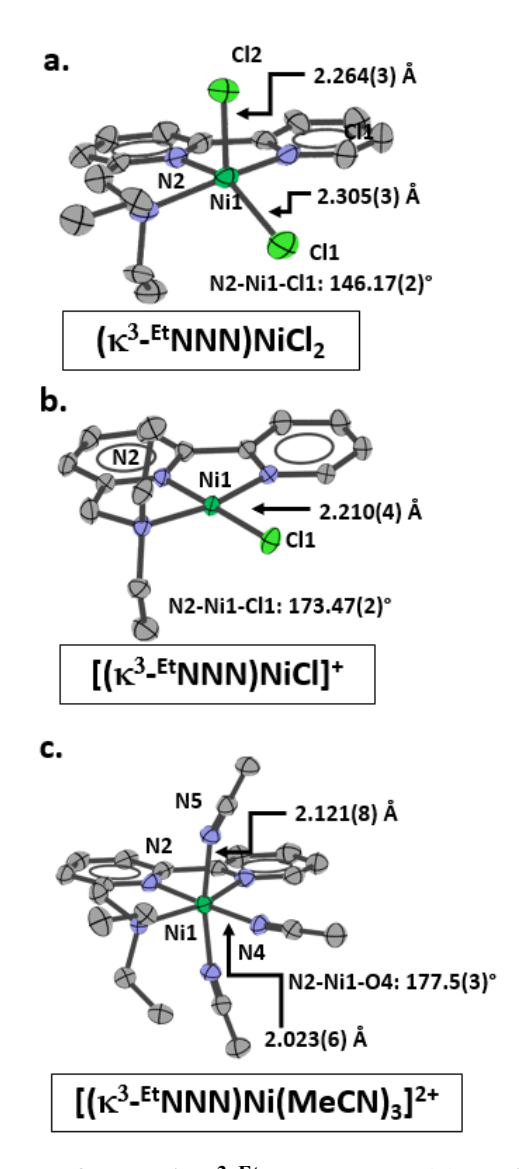


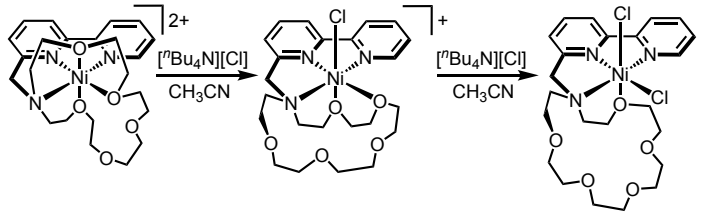
**Figure 3.** Structural representations of neutral  $(\kappa^3$ -EtNNN)NiCl<sub>2</sub> (a), cationic  $[(\kappa^3$ -EtNNN)NiCl]<sup>+</sup> (b), and dicationic  $[(\kappa^3$ -EtNNN)Ni(MeCN)<sub>3</sub>]<sup>2+</sup> (c), with ellipsoids at 50% and hydrogen atoms and anions omitted. See Supporting Information for full details.

The series of nickel complexes establishes the ability of the <sup>18c6</sup>NNN ligand to adopt a variety of coordination modes, a "flexidentate" character that allows the ligand to adapt its denticity to complete the octahedral coordination sphere. It is rare for a single ligand to support so many different coordination modes. Unlike the macrocyclic complexes with additional donors, the diethylamino variant cannot adopt multiple binding modes.

# **Interconversion of Ligand Binding Modes**

Given the coordinative flexibility of the the aza-crown ether macrocycle in the neutral, cationic and dicationic series, we were interested to see whether it was possible to interconvert between the ligand binding modes in solution. Double halide abstraction from (κ<sup>4</sup>-18c6NNN)NiCl<sub>2</sub> provided [(18c6NNN)Ni][OTf]<sub>2</sub>; adding tetrabutylammonium chloride salts stepwise reversed the process to furnish the mono- and dichloride complexes (Scheme 3, SI Figure 12), demonstrating the reversibility of the flexidentate characteristics.

**Scheme 3.** Reversing coordination mode changes by chloride addition.



Strong donor solvents such as acetonitrile can also coordinate to nickel and alter the denticity of the crown ether. Addition of MeCN to  $(\kappa^4$ - $^{18c6}$ NNN)NiCl<sub>2</sub> resulted in no observable change in the  $^{1}$ H NMR spectrum (SI Figure 13), and crystals grown from MeCN/ether gave the same unit cell for the structure shown in Figure 2a above, suggesting that the nitrile cannot displace the chelating ether ligand. Addition of MeCN to  $[(\kappa^5$ - $^{18c6}$ NNN)NiCl]<sup>+</sup> and  $[(\kappa^6$ - $^{18c6}$ NNN)Ni]<sup>2+</sup>, in contrast, leads to shifts in the paramagnetic resonances observed by  $^{1}$ H NMR spectroscopy consistent with nitrile coordination (SI Figures 14-16). Water exposure to  $[(\kappa^5$ - $^{18c6}$ NNN)NiCl]<sup>+</sup> also leads to coordination, forming a cationic tetradentate complex  $[(\kappa^4$ - $^{18c6}$ NNN)NiCl $(OH_2)]^+$  which was crystallographically characterized (Figure 4). The H<sub>2</sub>O ligand engages in hydogen bonding interactions with the macrocycle.

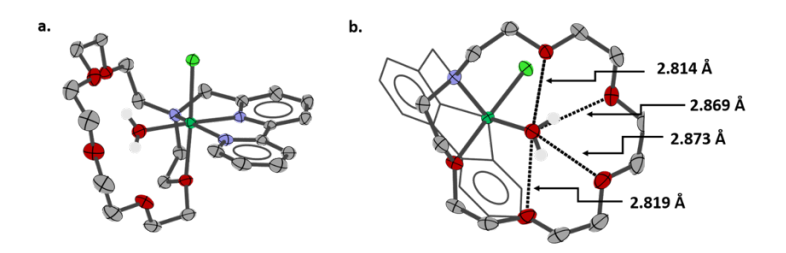


**Figure 4.** Structural representation of  $[(\kappa^{4}-18c6NNN)NiCl(OH_2)]^+$ , with ellipsoids at 50% and hydrogen atoms (except on aquo ligand) and anions omitted (a). Perspective highlighting the hydrogen bonding interactions between the aquo ligand and crown ether (b).

# Cyclic voltammetry

Given the extensive application of nickel bipyridine complexes in redox transformations, we aimed to characterize the reduction potentials of our new nickel complexes in acetonitrile solvent. To simplify the system, we focused on the dicationic complexes, which lack halide ligands that often dissociate upon reduction.<sup>34</sup> To ensure full acetonitrile solubility of nickel complexes and electrolyte, the bis(trifluoromethanesulfonyl)imide (NTf<sub>2</sub>) counteranion was used. The synthetic details for preparing NTf<sub>2</sub> salts of the nickel complexes are provided in the Supporting Information.

Cyclic voltammograms of both the macrocyclic and diethylamino complexes displayed three features (**Figure 5**). Scanning cathodically from the open circuit potential, the first reduction is assigned as the Ni<sup>II/I</sup> redox couple (see **SI Figures 23, 25** for Randles-Sevcik plots). The feature for  $[(\kappa^3-E^tNNN)Ni(MeCN)_3]^{2+}$  (bottom) was shifted anodically about 170 mV from  $[(\kappa^6-I^8c^6NNN)Ni]^{2+}$  (top). Potentials of the isolated first feature agree well with the full sweep shown in **Figure 5** (**SI Figures 27, 32**).

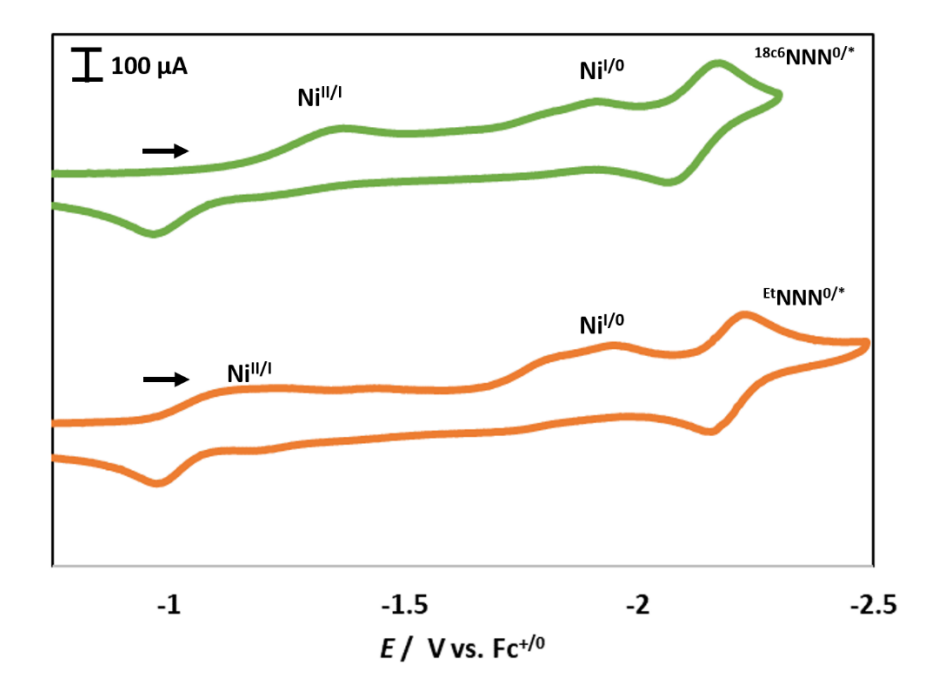


**Figure 5.** Cyclic voltammograms of 1 mM [( $^{18c6}NNN$ )Ni][NTf<sub>2</sub>]<sub>2</sub> (top) and [( $\kappa^3$ - $^{Et}NNN$ )Ni(MeCN)][NTf<sub>2</sub>]<sub>2</sub> (bottom) in acetonitrile with a 1.5 V/s scan rate and applied voltage corrected for ohmic drop. Glassy carbon working electrode, Pt wire counter electrode, Ag wire pseudoreference electrode. Referenced to Fc<sup>+/0</sup> with ferrocene internal standard.

The second redox feature displays two irreversible waves within 110 mV, labelled 2<sub>i</sub> and 2<sub>ii</sub> (**Figure 6**). Unlike the first reduction feature, the peak potentials for this second feature are very similar between the diethylamino and macrocyclic variant. Scan-rate dependent voltammetry of [(<sup>18c6</sup>NNN)Ni][NTf<sub>2</sub>]<sub>2</sub> reveals the more cathodic feature (2<sub>ii</sub>) increases in current as the scan rate increases (green to black, **Figure 6**), indicative of an EC mechanism. Finally, a third, reversible feature is assigned as the reduced ligand: in both cases the E<sub>1/2</sub> is shifted anodically from the free ligand by about 400 mV, as expected upon ligation to the Ni center.<sup>35,36</sup>

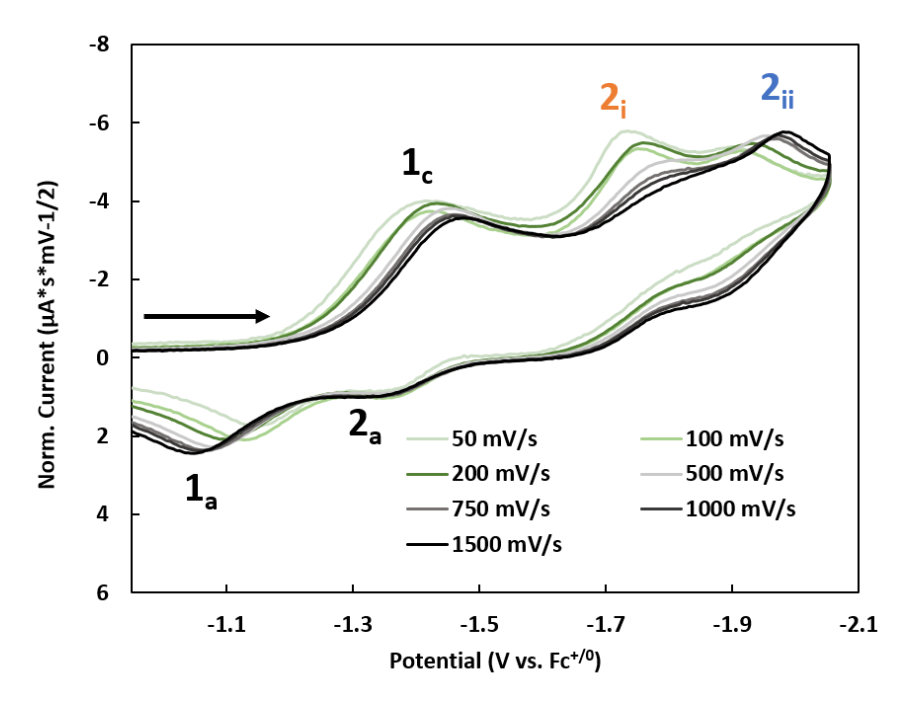


Figure 6. Scan-rate normalized cyclic voltammograms of the second redox feature of [(18c6NNN)Ni][NTf<sub>2</sub>]<sub>2</sub>(a).

## **Conclusions**

We report a new family of Ni(II) pincer complexes: three containing a flexible bipyridine-crown ether ligand capable of adopting  $\kappa^4$ ,  $\kappa^5$ , and  $\kappa^6$  coordination modes, and three diethylamino complexes without this capability. Reversible changes to the ligand denticity are possible through addition/removal of chloride ligands. Furthermore, the dicationic complexes are electrochemically characterized to reveal an EC mechanism indicating changes to the coordination sphere upon reduction and confirming the redox activity of the ligand.

## Acknowledgements

The material is based upon work supported by the National Science Foundation under grant no. CHE-2102244. We thank Brandie M. Ehrmann and the University of North Carolina at Chapel Hill Department of Chemistry Mass Spectrometry Core Laboratory, acknowledging support from the National Science Foundation under Grant No. CHE-1828183. E.Z.H. was partly supported by

the SURF program at the University of North Carolina at Chapel Hill. Some of the crystallographic work was supported by the National Science Foundation under grant no. CHE-2117287. E.Z.H. would like to thank Jillian Dempsey, Megan Jackson, and Alex Peroff for useful instruction during Cyclic Voltammetry Bootcamp at UNC Chapel Hill.

#### References

- (1) Constable, E. C.; Housecroft, C. E. The Early Years of 2,2'-Bipyridine—A Ligand in Its Own Lifetime. *Molecules* **2019**, *24* (21), 3951. https://doi.org/10.3390/molecules24213951.
- (2) Kaes, C.; Katz, A.; Hosseini, M. W. Bipyridine: The Most Widely Used Ligand. A Review of Molecules Comprising at Least Two 2,2'-Bipyridine Units. *Chem. Rev.* **2000**, *100* (10), 3553–3590. https://doi.org/10.1021/cr990376z.
- (3) Rubtsov, A. E.; Malkov, A. V. Recent Advances in the Synthesis of 2,2'-Bipyridines and Their Derivatives. *Synthesis* **2021**, *53* (15), 2559–2569. https://doi.org/10.1055/s-0040-1706030.
- (4) Smith, A. P.; Fraser, C. L. 1.1 Bipyridine Ligands. In *Comprehensive Coordination Chemistry II*; McCleverty, J. A., Meyer, T. J., Eds.; Pergamon: Oxford, 2003; pp 1–23. https://doi.org/10.1016/B0-08-043748-6/01103-8.
- (5) Wenger, O. S. Photoactive Nickel Complexes in Cross-Coupling Catalysis. *Chem. Eur. J.* **2021**, *27* (7), 2270–2278. https://doi.org/10.1002/chem.202003974.
- (6) Cagan, D. A.; Bím, D.; Kazmierczak, N. P.; Hadt, R. G. Mechanisms of Photoredox Catalysis Featuring Nickel–Bipyridine Complexes. *ACS Catal.* **2024**, *14* (11), 9055–9076. https://doi.org/10.1021/acscatal.4c02036.
- (7) Tasker, S. Z.; Standley, E. A.; Jamison, T. F. Recent Advances in Homogeneous Nickel Catalysis. *Nature* **2014**, *509* (7500), 299–309. https://doi.org/10.1038/nature13274.
- (8) Palkowitz, M. D.; Emmanuel, M. A.; Oderinde, M. S. A Paradigm Shift in Catalysis: Electro- and Photomediated Nickel-Catalyzed Cross-Coupling Reactions. *Acc. Chem. Res.* **2023**, *56* (20), 2851–2865. https://doi.org/10.1021/acs.accounts.3c00479.
- (9) Olivier-Bourbigou, H.; Breuil, P. A. R.; Magna, L.; Michel, T.; Espada Pastor, M. F.; Delcroix, D. Nickel Catalyzed Olefin Oligomerization and Dimerization. *Chem. Rev.* **2020**, *120* (15), 7919–7983. https://doi.org/10.1021/acs.chemrev.0c00076.
- (10) Desage-El Murr, M. Anatomy of a Redox-Active Ligand. In *Redox-Active Ligands*; John Wiley & Sons, Ltd, 2024; pp 1–20. https://doi.org/10.1002/9783527830879.ch1.
- (11) Chirik, P. J. Preface: Forum on Redox-Active Ligands. *Inorg. Chem.* **2011**, *50* (20), 9737–9740. https://doi.org/10.1021/ic201881k.
- (12) Lappin, A. G.; McAuley, A. The Redox Chemistry of Nickel. In *Advances in Inorganic Chemistry*; Sykes, A. G., Ed.; Academic Press, 1988; Vol. 32, pp 241–295. https://doi.org/10.1016/S0898-8838(08)60233-0.
- (13) Lin, Q.; Dawson, G.; Diao, T. Experimental Electrochemical Potentials of Nickel Complexes. *Synlett* **2021**, *32* (16), 1606–1620. https://doi.org/10.1055/s-0040-1719829.
- (14) Dawson, G. A.; Lin, Q.; Neary, M. C.; Diao, T. Ligand Redox Activity of Organonickel Radical Complexes Governed by the Geometry. *J. Am. Chem. Soc.* **2023**, *145* (37), 20551–20561. https://doi.org/10.1021/jacs.3c07031.

- (15) Paretzki, A.; Bubrin, M.; Fiedler, J.; Záliš, S.; Kaim, W. Correlated Coordination and Redox Activity of a Hemilabile Noninnocent Ligand in Nickel Complexes. *Chem. Eur. J.* **2014**, *20* (18), 5414–5422. https://doi.org/10.1002/chem.201304316.
- (16) Acosta-Calle, S.; Miller, A. J. M. Tunable and Switchable Catalysis Enabled by Cation-Controlled Gating with Crown Ether Ligands. *Acc. Chem. Res.* **2023**, *56* (8), 971–981. https://doi.org/10.1021/acs.accounts.3c00056.
- (17) Yoo, C.; Dodge, H. M.; Miller, A. J. M. Cation-Controlled Catalysis with Crown Ether-Containing Transition Metal Complexes. *Chem. Commun.* **2019**, *55* (35), 5047–5059. https://doi.org/10.1039/C9CC00803A.
- (18) Kita, M. R.; Miller, A. J. M. Cation-Modulated Reactivity of Iridium Hydride Pincer-Crown Ether Complexes. *J. Am. Chem. Soc.* **2014**, *136* (41), 14519–14529. https://doi.org/10.1021/ja507324s.
- (19) Gregor, L. C.; Grajeda, J.; Kita, M. R.; White, P. S.; Vetter, A. J.; Miller, A. J. M. Modulating the Elementary Steps of Methanol Carbonylation by Bridging the Primary and Secondary Coordination Spheres. *Organometallics* **2016**, *35* (17), 3074–3086. https://doi.org/10.1021/acs.organomet.6b00607.
- (20) Grajeda, J.; Kita, M. R.; Gregor, L. C.; White, P. S.; Miller, A. J. M. Diverse Cation-Promoted Reactivity of Iridium Carbonyl Pincer-Crown Ether Complexes. *Organometallics* **2016**, *35* (3), 306–316. https://doi.org/10.1021/acs.organomet.5b00786.
- (21) Kita, M. R.; Miller, A. J. M. An Ion-Responsive Pincer-Crown Ether Catalyst System for Rapid and Switchable Olefin Isomerization. *Angew. Chem. Int. Ed.* **2017**, *56* (20), 5498–5502. https://doi.org/10.1002/anie.201701006.
- (22) Smith, J. B.; Miller, A. J. M. Connecting Neutral and Cationic Pathways in Nickel-Catalyzed Insertion of Benzaldehyde into a C–H Bond of Acetonitrile. *Organometallics* **2015**, *34* (19), 4669–4677. https://doi.org/10.1021/acs.organomet.5b00405.
- (23) Smith, J. B.; Kerr, S. H.; White, P. S.; Miller, A. J. M. Thermodynamic Studies of Cation–Macrocycle Interactions in Nickel Pincer–Crown Ether Complexes Enable Switchable Ligation. *Organometallics* **2017**, *36* (16), 3094–3103. https://doi.org/10.1021/acs.organomet.7b00431.
- (24) Farquhar, A. H.; Gardner, K. E.; Acosta-Calle, S.; Camp, A. M.; Chen, C.-H.; Miller, A. J. M. Cation-Controlled Olefin Isomerization Catalysis with Palladium Pincer Complexes. *Organometallics* **2022**, *41* (22), 3366–3372. https://doi.org/10.1021/acs.organomet.2c00315.
- (25) Acosta-Calle, S.; Huebsch, E. Z.; Kolmar, S. S.; Whited, M. T.; Chen, C.-H.; Miller, A. J. M. Regulating Access to Active Sites via Hydrogen Bonding and Cation–Dipole Interactions: A Dual Cofactor Approach to Switchable Catalysis. *J. Am. Chem. Soc.* **2024**, *146* (16), 11095–11104. https://doi.org/10.1021/jacs.3c10877.
- (26) Thaler, A.; Bergter, R.; Ossowski, T.; Cox, B. G.; Schneider, H. Synthesis and Silver(I) Coordination of N-Functionalized Aza-Crown Ethers with Pendant Aromatic Carbocyclic or Heterocyclic Side-Arms. *Inorg. Chim. Acta* **1999**, *285* (1), 1–9. https://doi.org/10.1016/S0020-1693(98)00253-9.
- (27) Kira, J.; Ossowski, T. An Influence of 2,2'-Bipyridine Side-Arm on Complexation Equilibria of Monoaza Crown Ethers in Various Solvents. *Pol. J. Chem.* **2008**, No. Vol. 82, nr 6, 1245–1254.
- (28) King, R. P.; Yang, J. Y. Modular Preparation of Cationic Bipyridines and Azaarenes *via* C–H Activation. *Chem. Sci.* **2023**, *14* (46), 13530–13536. https://doi.org/10.1039/D3SC04864K.

- (29) Deutsch, J. L.; Poling, S. M. The Determination of Paramagnetic Susceptibility by NMR: A Physical Chemistry Experiment. *J. Chem. Educ.* **1969**, *46* (3), 167. https://doi.org/10.1021/ed046p167.
- (30) Irwin, M.; Doyle, L. R.; Krämer, T.; Herchel, R.; McGrady, J. E.; Goicoechea, J. M. A Homologous Series of First-Row Transition-Metal Complexes of 2,2'-Bipyridine and Their Ligand Radical Derivatives: Trends in Structure, Magnetism, and Bonding. *Inorg. Chem.* 2012, 51 (22), 12301–12312. https://doi.org/10.1021/ic301587f.
- (31) Wang, M.; England, J.; Weyhermüller, T.; Wieghardt, K. Electronic Structures of "Low-Valent" Neutral Complexes [NiL2]0 (S = 0; L = Bpy, Phen, Tpy) An Experimental and DFT Computational Study. *Eur. J. Inorg. Chem.* **2015**, *2015* (9), 1511–1523. https://doi.org/10.1002/ejic.201403144.
- (32) Smith, J. B.; Camp, A. M.; Farquhar, A. H.; Kerr, S. H.; Chen, C.-H.; Miller, A. J. M. Organometallic Elaboration as a Strategy for Tuning the Supramolecular Characteristics of Aza-Crown Ethers. *Organometallics* **2019**, *38* (22), 4392–4398. https://doi.org/10.1021/acs.organomet.9b00462.
- (33) Addison, A. W.; Rao, T. N.; Reedijk, J.; Rijn, J. van; Verschoor, G. C. Synthesis, Structure, and Spectroscopic Properties of Copper(II) Compounds Containing Nitrogen—Sulphur Donor Ligands; the Crystal and Molecular Structure of Aqua[1,7-Bis(N-Methylbenzimidazol-2'-Yl)-2,6-Dithiaheptane]Copper(II) Perchlorate. *J. Chem. Soc., Dalton Trans.* **1984**, No. 7, 1349–1356. https://doi.org/10.1039/DT9840001349.
- (34) Kariofillis, S. K.; Doyle, A. G. Synthetic and Mechanistic Implications of Chlorine Photoelimination in Nickel/Photoredox C(Sp3)–H Cross-Coupling. *Acc. Chem. Res.* **2021**, 54 (4), 988–1000. https://doi.org/10.1021/acs.accounts.0c00694.
- (35) Budnikova, Yu. G.; Yakhvarov, D. G.; Morozov, V. I.; Kargin, Yu. M.; Il'yasov, A. V.; Vyakhireva, Yu. N.; Sinyashin, O. G. Electrochemical Reduction of Nickel Complexes with 2,2'-Bipyridine. *Russ. J. Gen. Chem.* **2002**, *72* (2), 168–172. https://doi.org/10.1023/A:1015401029839.
- (36) Derien, S.; Dunach, E.; Perichon, J. From Stoichiometry to Catalysis: Electroreductive Coupling of Alkynes and Carbon Dioxide with Nickel-Bipyridine Complexes. Magnesium Ions as the Key for Catalysis. *J. Am. Chem. Soc.* **1991**, *113* (22), 8447–8454. https://doi.org/10.1021/ja00022a037.